Pol. J. Environ. Stud. Vol. 33, No. 4 (2024), 4551-4559
DOI: 10.15244/pjoes/176057 ONLINE PUBLICATION DATE: 2024-05-20

Original Research

Beta vulgaris L. Extract Mediated Biogenic Synthesis of Magnesium Oxide Nanostructures and their Enhanced Antibacterial, Antioxidant, and Cytocompatibility Activities

Tanu Dixit, Jitendra Suthar, Selvan Ravindran*

Symbiosis School of Biological Sciences, Faculty of Medical and Health Sciences, Symbiosis International (Deemed University), Lavale, Pune

Received: 9 September 2023
Accepted: 28 November 2023

Abstract

Metal oxide nanostructures have lately sparked a lot of interest owing to their high stability. However, chemical synthesis of these compounds necessitates the use of costly, toxic, and hazardous chemicals. This study involves the biosynthesis of magnesium oxide nanostructures (Nano-MgO) using *Beta vulgaris* extract (BVE) as a reducing agent in a simple and environmentally friendly way. Preliminary investigations were used to assess the phytochemicals present in the prepared BVE. The synthesized nanostructures were characterized by UV visible spectroscopy, SEM-EDX, XRD, FTIR, TGA, and DSC. The Nano-MgO absorption peak was observed at a wavelength of 270 nm. SEM studies showed a mean particle size of about 36.28 nm and EDX analysis revealed the presence of magnesium and oxygen in weight percentages of 27% and 72% respectively. XRD demonstrated the crystalline and cubic nature of synthesized Nano-MgO. FTIR verified Nano-MgO vibrational frequency at 565.07 cm^{-1}. Antioxidant assay (ABTS) revealed that Nano-MgO exhibited higher antioxidant activity than BVE alone. Significant antibacterial effects were demonstrated by Nano-MgO, with a substantial inhibition zone against *Escherichia coli* (3.8 cm) *Staphylococcus aureus* (3.9 cm). The cytotoxic impact of Nano-MgO on PC-12 cell lines revealed the IC-50 value to be 30.94 µg/mL for 24 hours of incubation.

Keywords: *Beta vulgaris* extract, nanostructures, biosynthesis, antioxidant activity, antibacterial activity, eco-friendly synthesis

*e-mail: selvan_ravindran@yahoo.com

Introduction

Nanoscale has become extremely significant for a multitude of reasons, the most notable of which is that it enhances the surface-to-volume ratio found in most nanoscale components when compared to bulk materials of the same materials. This is because the number of atoms, ions, or molecules that make up a nanoparticle increases on its surface rather than within it. Nanotechnology is the study of microscopic structures with sizes between 0.1 and 100 nm [1, 2]. As a result, different nanoparticles with specific traits arise, and the nanoparticles display diverse chemical, physical, and biological attributes at the nanoscale compared to their respective particles at larger sizes. This field of material science has great potential that can create a wide range of materials at the nanoscale level with numerous applications in almost every field, including electronics, sunscreens, cosmetics, biolabeling, catalysis, renewable energy, environmental remediation, and medicine, among others [3, 4]. Many areas of material, physics, and chemical science depend on metal oxides, as they are smaller than other materials and have a highly dense edge surface, which might allow them to display peculiar chemical or physical traits. Furthermore, owing to their higher surface- to-volume ratio, metal oxides at the nanoscale exhibit greatly improved and novel magnetic, electrical, and catalytic capabilities as compared to traditional bulk metals.

Metal oxide-based nanoparticles are intriguing due to their structural characteristics, notably network symmetry and unit parameters [5, 6]. As a result of the rise in antibiotic-resistant strains and infectious diseases, metal nanoparticles have a broader variety of biopharmaceutical and biomedical applications as substitute antibacterial agents [7]. New nano-based materials are being synthesized and implemented into everyday personal care products, pharmaceuticals, cosmetics, and drug delivery to influence the manufacturing and industrial sectors. The commercial applications of nanomaterials and the development of nano-based devices will continue to grow with regulated synthesis [8]. Metallic nanomaterials have been fabricated employing several biological techniques, such as utilizing enzymes, bacteria, and plant components, which are thought to be effective eco-friendly nano-factories [9]. The interaction of metals with microbes or plant extracts has been employed in various applications, including biomineralization, bioremediation, bioleaching, and biocorrosion. As a result, nanoparticle biosynthesis has emerged as a potential study area in nanobiotechnology, linking biotechnology, and nanotechnology [10].

Plant-mediated synthesis is one of the biological techniques, which is most straightforward, dependable, cost-effective, and non-toxic [11]. Plants include phytochemicals, such as proteins, polysaccharides, flavonoids, tannins, ketones, alcohols, and others that work as excellent reducing agents in the required characteristics [12, 13]. Nanostructured magnesium oxide offers a broad range of applications owing to its distinct characteristics, including high band gap, low refractive index, and thermodynamic stability [14].

It has been employed for many purposes, including catalysis, hazardous waste removal, refractory materials, additives in heavy fuel oils, absorbents, superconductive thin films as a substrate for superconductors, and more [15].

Magnesium oxide nanoparticles (MgO-NPs) are white powders with a high melting point that is odorless and harmless. According to previous studies, the bactericidal effectiveness of MgO-NPs increases as particle size and concentration decrease [16]. MgO-NPs are a safe antibacterial agent that is relatively easy to obtain among many different inorganic metal oxides. They can alleviate heartburn, stimulate the activation of bone repair scaffolds, and function as an anticancer agent. MgO-NPs were identified as a potential candidate as they are biocompatible, environment-friendly, and safe for various human cell lines, making them appropriate for biomedical applications [17]. MgO-NPs coated with polyethylene glycol have also been used as a delivery agent for anticancer medications like 2-methoxy estradiol, demonstrating their value in regulated drug delivery systems [18]. Recent breakthroughs in nanomaterials and nanomedicine have resulted in significant developments with enormous promise.

Beetroot is a common agricultural crop of the Chenopodiaceae family, and its root is essential in sugar production. Swedish botanist "Linnaeus (Carl Linne, 1707-1778)" described *B. vulgaris* L. in 1753 [19]. It is a vitamin-rich vegetable that is widely accessible and includes a variety of beneficial chemicals such as manganese, folate, and magnesium. Beetroot pigments are water soluble and are impacted by a range of factors such as pH, moisture, temperature, light, and oxygen. Beetroots are used in traditional medicine to cure a variety of ailments. Their effects include antidepressant, immunostimulant, antihypertensive, antioxidant, antihyperlipidemic, radioprotective, and hepatoprotective activities [20]. Because of its high sugar content, beetroot has a high reductive capability that can be exploited to synthesize nanomaterials. It also comprises phytochemicals such as betalains, known as betaxanthins and betacyanins, as well as polyphenolics and flavonoids, which have been utilized as capping and reducing agents in the preparation of gold and zinc oxide nanoparticles.

In this study, a sustainable and environmentally friendly method based on biological synthesis principles has been developed for the synthesis of magnesium oxide nanostructures (Nano-MgO). *B. vulgaris* L. extract, also known as beetroot extract, which has great medicinal capabilities was utilized as a reducing agent [21]. The effective synthesis of Nano-MgO was confirmed by characterization methods including UV-vis spectroscopy, SEM-EDX, FTIR, XRD, TGA, and DSC analysis. Moreover, the study also showed that

these nanostructures have the potential to be used as an antioxidant and antibacterial agent.

Materials and Methods

Analytical-grade chemicals of the highest purity were employed in the current study. The beetroots (*B. vulgaris* L.) used for biosynthesis in the study were procured from the local market in Pune, India. The plant name was identified as *B. vulgaris* L. and belongs to the family Amaranthaceae authenticated by the "Botanical Survey of India, Western Regional Centre, Pune, Government of India." The beetroot (59 g) was cleaned with tap water and rinsed with deionized water to eliminate dust and particle pollutants. It was then dried, peeled, chopped and ground in a household blender with 250 mL deionized water and further heated for 2 hours at 60ºC. After allowing it to cool to ambient temperature and filtering it with Whatman filter paper, 200 mL of the extract was obtained and stored in the refrigerator at 5-10ºC for future use.

UV-visible analysis was done by using a Shimadzu U.V-1900 U.V spectrophotometer. The morphology, size, and elemental analyses of biosynthesized nanostructures were determined using "Scanning Electron Microscopy" (SEM) in conjunction with "Energy-Dispersive X-ray Analysis" (EDX). To analyze the crystalline structure of Nano -MgO (=1.541), "X-ray diffraction" (XRD) patterns were acquired using a D8 ADVANCE-D8X XRD system (Bruker) with a Cu Kline as the source of radiation [22]. "Fourier Transform Infrared" (FTIR) analysis was performed using a Bruker Alpha spectrometer and the software OPUS7 to analyze the presence of Mg-O bonds and other functional groups in the prepared sample. "Thermogravimetric analysis" (TGA) was used to examine materials by calculating mass change as a function of temperature and "Differential scanning calorimetry" was done to study the thermal properties of synthesized Nano-MgO.

Synthesized nanostructures were assessed for antioxidant activity where BVE and synthesized Nano-MgO at varied concentrations of 50, 100, 150, 200, 250, and 500 g/mL were independently tested by a standard approach utilizing a sigma antioxidant assay kit (Catalogue Number- CS0790) [23]. A plate reader was used to determine endpoint absorbance at 620 nm. Also, the antimicrobial activity of the nanostructures was assessed utilizing well diffusion method against *E. coli* and *S. aureus* by taking BVE and Nano-MgO as test samples, and standard commercial antibiotic gentamicin and ciprofloxacin as positive controls [24]. PC-12 cells were obtained from NCCS Pune, India. MTT "3-[4,5-dimethylthiazol-2-yl]-2,5 diphenyl tetrazolium bromide" assay was performed to access the cell viability where PC-12 cells were exposed for 24, 48, 72, and 96 hrs. to various concentrations of Nano-MgO including 0.1, 0.5, 1, 5, 10, 25, 50 and 100 µg/mL.

Identification of Phytonutrients

Standard preliminary tests were performed to determine the phytonutrients present in the prepared BVE responsible for the process of reduction to synthesize the Nano-MgO. The presence of biologically active compounds such as phenols, flavonoids, saponins, sterols, terpenoids and tannins was studied according to the established protocols [25, 26].

Biological Synthesis of Nano-MgO

200 mL of MgCl2 .6H2O (0.5M) was dissolved in Milli-Q water to obtain an aqueous solution to which *B. vulgaris* extract (50 mL) was gradually added under continuous stirring and heating (70ºC) for about 5 hours. The completion of the reaction and synthesis of the Nano-MgO was indicated by the solution's color changing from dark pink to green and the reaction was stopped and mixture was transferred to falcon tubes for centrifugation. After centrifugation at 7000 rpm for 7 minutes, the precipitate was washed three times with ethanol to eliminate free magnesium oxide associated with Nano-MgO. Then the pellet was separated from the supernatant and dried for 3 hours at 75°C in a hot air oven. After drying, the sample was crushed by utilizing mortar and pestle to obtain white powder [27, 28]. Yield of the biosynthesized Nano-MgO was approximately fifty-seven percent.

Results and Discussion

Investigation of Phytochemicals

In an aqueous BVE, the phytonutrients that help synthesize and cap Nano-MgO from the magnesium oxide precursor are qualitatively investigated. The phytochemical screening of the aqueous BVE (Fig. 1) demonstrated that it is an excellent source of secondary metabolites such as phenols, flavonoids, saponins, sterols and tannins. These metabolites might be important in reducing magnesium chloride and the stability and synthesis of nanostructures. Further, the results showed the absence of terpenoids (Table 1) in the synthesized BVE since the extract was synthesized by heating at 60°C, where terpenoids are more volatile at high temperatures with enhanced emission from the pool.

U.V Visible Spectroscopy

In a UV-visible spectrophotometer, the absorption spectra of the synthesized Nano-MgO were recorded between 200 and 700 nm (Fig. 2a). The strong peak at λmax 270 nm confirmed their nanoscale size, restricted particle size distribution, and monodispersed nature. [29] For the developed Nano-MgO, Fig. 2b) shows the usual dependency of $(\alpha hv)^2$ v/s hυ where band gap energy

(Eg) is determined by the straight line's intersection with the h-axis. In comparison to bulk MgO, which had a predicted band gap energy of 7.8 eV using the Tauc plot and formula:

$$(\propto h\nu)^n = A\,(\,h\nu - E_g\,),$$

where Eg = Band gap, h = constant, Planck's and v = Frequency. By plotting $(\alpha h\nu)^2$ versus photon energy (h) and projecting the linear section of the curve to the photon energy axis we calculated the energy bandgap (Eg), which was 4.1 eV for synthesized Nano-MgO. This is in close agreement with the previous studies including *Citrus limon* (4.2 eV) [30] and *Hagenia abyssinica* (4.19 eV) [31]. The existence of 4-coordinated surface anions near the border of the Nano-MgO, as opposed to 6-coordinated surface anions in the bulk materials, is undoubtedly superintended for the band gap energy. Furthermore, the energy band gap could be influenced by the diameters of the MgO particles in the nano region, band gap energy increases as particle size decreases [32].

SEM-EDX Analysis

The topographical surface appearance, aggregation, and chemical composition of the produced Nano-MgO were studied by SEM-EDX analysis. SEM image (Fig. 3a) indicated that the particles of synthesized Nano-MgO are homogenous, spherical, uniform, and agglomerated with good size distribution. The calculated mean particle size is 36.28 nm. Moreover, the EDX analysis revealed the sample has the existence of magnesium and oxygen in weight percentages of 27% and 72%, respectively (Fig. 3b). It revealed that the sample has the required phases of Mg and O [33]. Furthermore, the emergence of peaks with energies between 0.5 and 1.5 KeV demonstrated the effective synthesis of Nano-MgO [33, 34]. Other peaks in the sample indicate the presence of contaminants, which XRD analysis later confirmed (Fig. 3b). According to studies, the appearance of extra peaks in the EDX profile was caused by the breakdown of enzymes, proteins, and other phytochemicals that function as stabilizers.

Table 1. Phytochemical analysis of synthesized *Beta vulgaris* extract.

Phytonutrients	Results
Phenols	+
Flavonoids	+
Saponins	+
Sterols	+
Terpenoids	-
Tannins	+

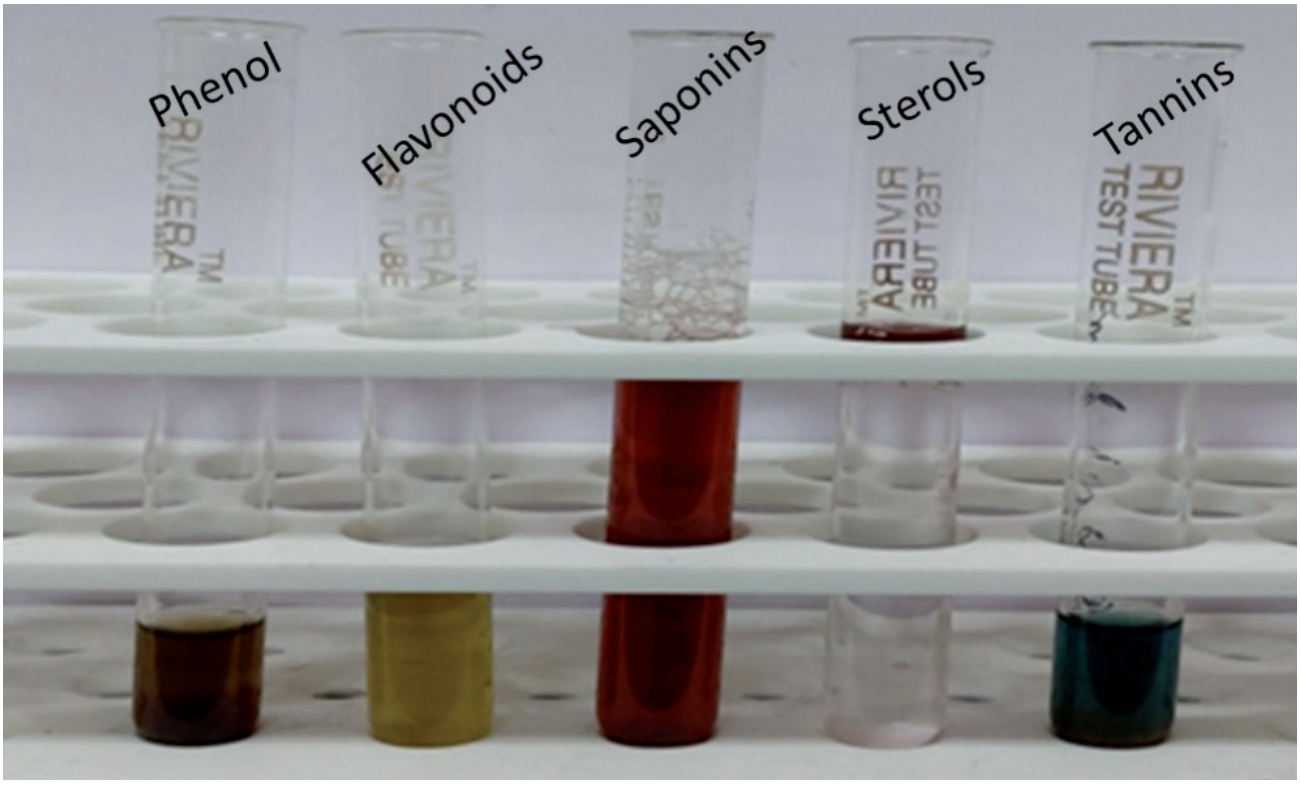

Fig. 1. The aqueous extract of *Beta vulgaris* was exposed to phytochemical screening tests, which identified the presence of phenols, flavonoids, saponins, sterols, and tannins. Notably, the extract was discovered to be devoid of terpenoids.

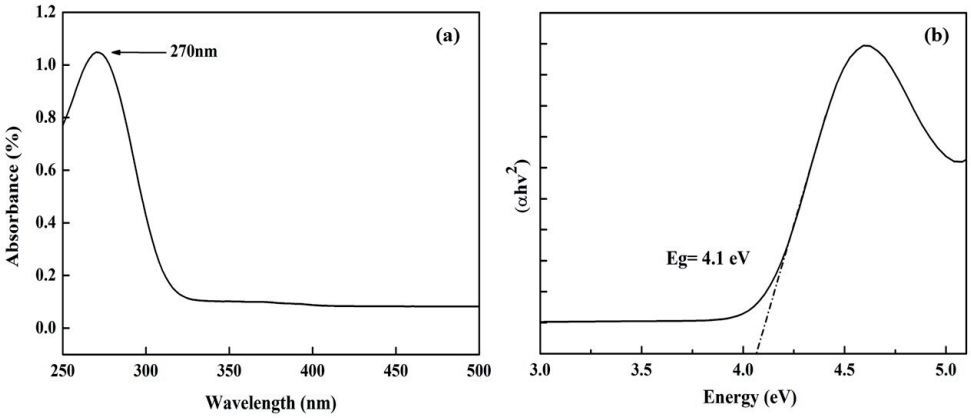

Fig. 2. The optical properties of synthesized Nano-MgO a) UV-Visible spectrum, and; b) Energy bandgap.

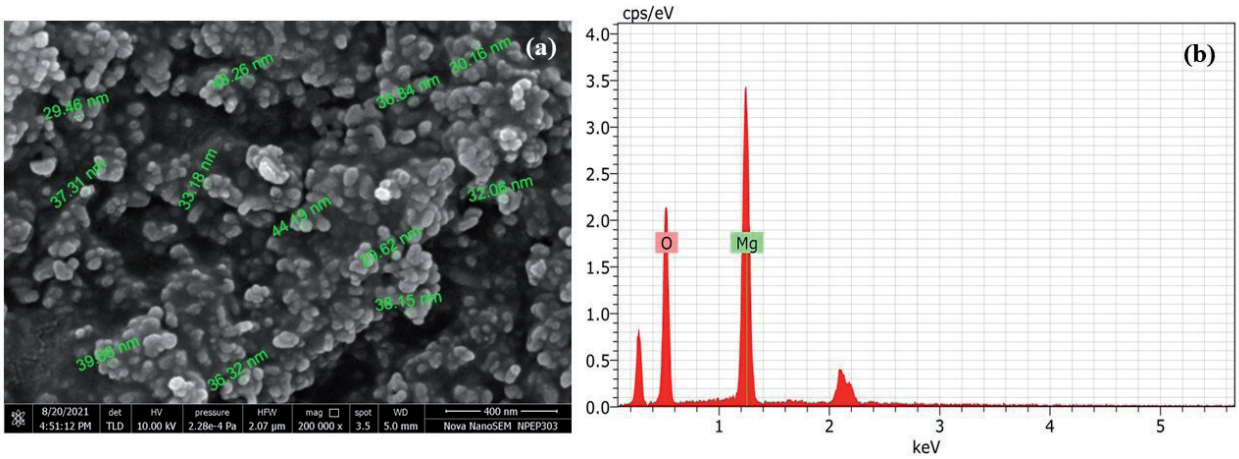

Fig. 3. Nano-MgO surface morphology and elemental composition analysis by; a) FE-SEM of Nano-MgO at resolution 400 nm. Mean particle size is 36.28±10 nm; b) EDX profile.

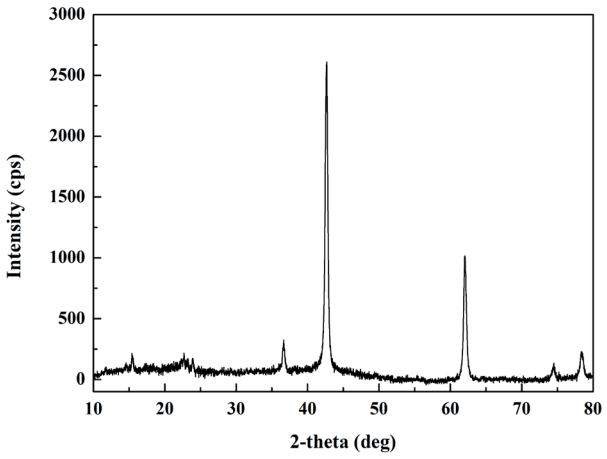

Fig. 4. XRD patterns of Nano-MgO for crystallographic structure analysis.

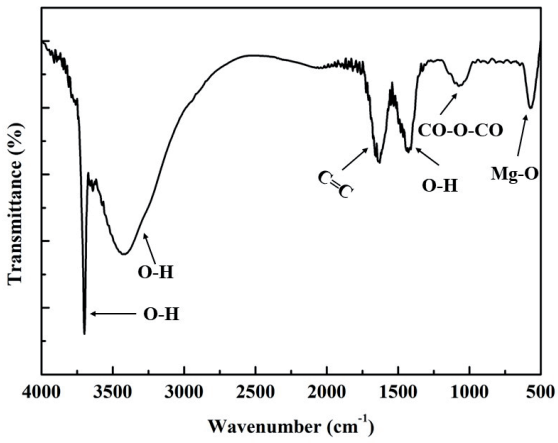

Fig. 5. FTIR of synthesized Nano-MgO for determination of functional groups.

XRD Analysis

Further, the crystalline nature and purity of the fabricated Nano-MgO were determined by employing an XRD study (Fig. 4). At 2θ intensity, five notable peaks are observed: 36.58°, 42.61°, 62°, 74.4°, and 78.3°, which corresponds to planes (1 1 1), (2 0 0), (2 2 0), (3 1 1), and (2 2 2), in the given order. These peak values are compared and matched with JCPDS standard file 89-7746, suggesting that the synthesized Nano-MgO

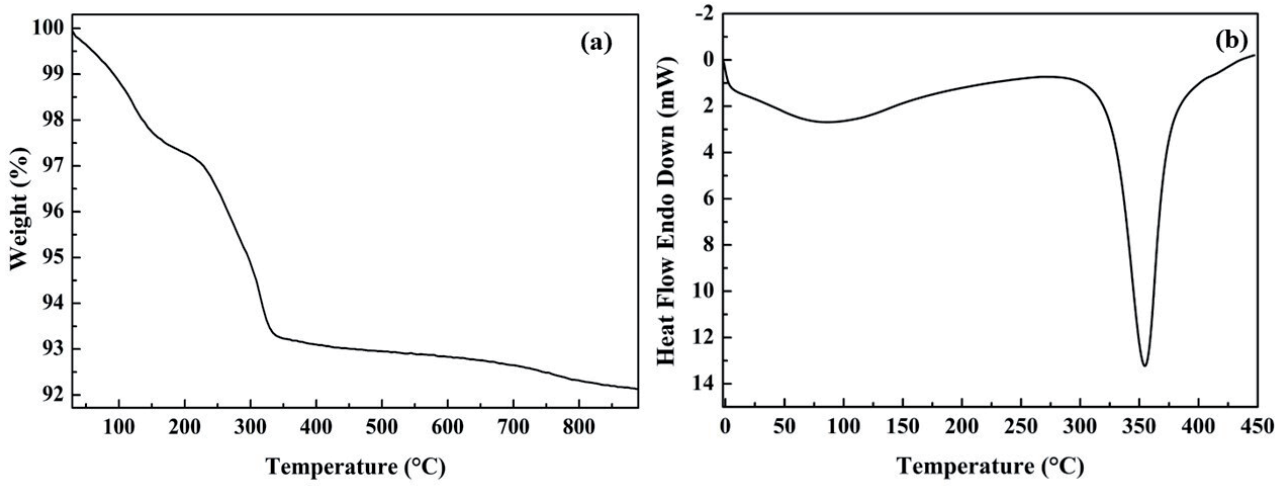

Fig. 6. a) Thermogram; b) Differential Scanning Calorimetry of Nano-MgO.

powder is crystalline and cubic [35, 36]. Furthermore, the presence of extra peaks in the XRD spectra verifies the findings from the EDX examination, which revealed that the sample included other forms of Nano-MgO. Using the Debye-Scherrer equation, the average crystallite size was calculated to be 23.32 nm by using the formula:

$$D = K\lambda/\beta cos\theta$$

Where D corresponds to "crystalline size," K corresponds to the "Scherer constant (0.9)", λ is taken as 1.5406 nm, β corresponds to the "full width at half maximum of the diffraction peak" and θ is the "angle of diffraction".

FTIR Spectroscopy

The occurrence of a functional group in the prepared Nano-MgO was determined using FT-IR analysis which showed the presence of absorption bands at 3698.98 cm^{-1}, 3427.18 cm^{-1}, 1635.80 cm^{-1}, and 565.07 cm^{-1} (Fig. 5). Observed C=C stretching vibration is related to the absorption band at 1635 cm^{-1}. Three peaks at 3698 cm^{-1}, 3639 cm^{-1}, and 3427 cm^{-1} correspond to the O-H stretch of the water, which is reabsorbed from the surrounding environment. Mg-O vibrations are responsible for the peak at 565.07 cm^{-1}. The existence of MgO at the nanoscale is demonstrated by the peaks ranging from 400 cm^{-1} to 700 cm^{-1} [37-39].

TGA and DSC

TGA measures the change in mass as a function of temperature to characterize materials, whereas DSC is a thermoanalytical approach that analyzes the variation in the amount of heat required to raise the temperature of a sample relative to a reference as a function of temperature. Here X-Axis is the temperature at which the sample was heated up to 900 degrees in the presence of nitrogen. Y-Axis was the Weight (%) or amount of compound lost, i.e., around 10% of adsorbed molecules on the surface are lost, and 90% of the compound is stable, as seen in the thermogram (Fig. 6a) [40]. Further, it is considered that the dehydration of hydroxyl groups on the brucite layers, which results in the production of MgO, is what causes the occurrence of a single massive endothermic transition (Td) at 360°C. According to this data, MgO particles can develop when the treatment temperature is lower than 360°C (Fig. 6b).

Antioxidant Activity

ABTS test was employed to investigate the antioxidant properties of prepared BVE and Nano-MgO *in-vitro*. The scavenging impact of the BVE and Nano-MgO on ABTS radicals (Fig. 7) was found to be significant and dose-dependent, where the Trolox reagent was employed as a control. In the instance of BVE, ABTS cation radical scavenging activity was 11-64% at

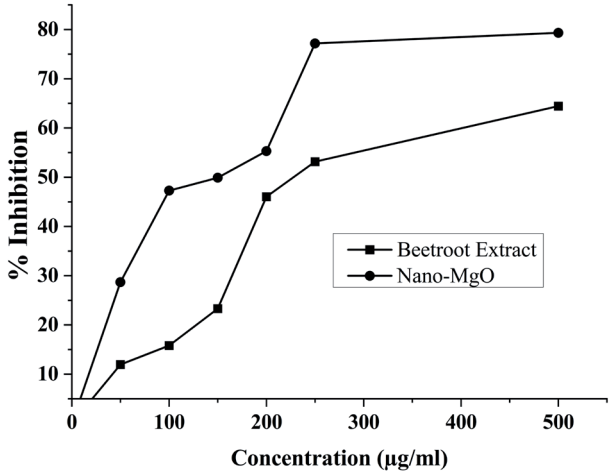

Fig. 7. Graph showing ABTS activity of *Beta vulgaris* extract and Nano-MgO.

a concentration range of 50-500 g/mL when compared to *B. vulgaris* section, it was 28-79% in the case of Nano-MgO, demonstrating that biosynthesized nanoparticles have more significant antioxidant properties [41, 42].

Antimicrobial Activity

S. aureus and *E. coli* bacteria were utilized to assess antibacterial activity by employing 1 mg of Nano-MgO (Fig. 8). In the presence of MgO nanoparticles, both bacteria demonstrated antibacterial action, but no discernible activity in the presence of BVE. The findings demonstrated that Nano-MgO had a high inhibition efficacy against both microbial pathogens, with the zone inhibition diameter against S. aureus measuring 3.9 cm as opposed to 3.4 cm for ciprofloxacin as a control. The inhibition effects of Nano-MgO against *E. coli* were at 3.8 cm compared to control gentamicin at 3.4 cm.

Cell Viability

MTT assay was utilized to evaluate the percent viability of PC-12 cells treated with different concentrations of Nano-MgO (0.5-100 µg/mL), and the findings were analyzed using Two-Way-ANNOVA and software called graph pad prism 6.0. Nano-MgO alone causes a decrease in cell viability as time and concentration increase (Fig 9a). When evaluating the effect of nanoparticles on cell viability, a 40 percent decline in cell viability at 100 g/mL concentration occurs after 24 hours, and a significant loss in cell viability occurs after 48, 72, and 96 hours at concentrations over 25 µg/mL, as compared to control. The logIC50 of Nano-MgO at different time points was also calculated (Fig. 9b) and was found to be 30.94 µg/mL for 24 hrs., 14.08 µg/mL for 48 hrs., and 11.03 µg/mL for 72 hrs. and 10.49 µg/mL for 96 hrs. Our data showed that the logIC50 value decreases with an increase in incubation time.

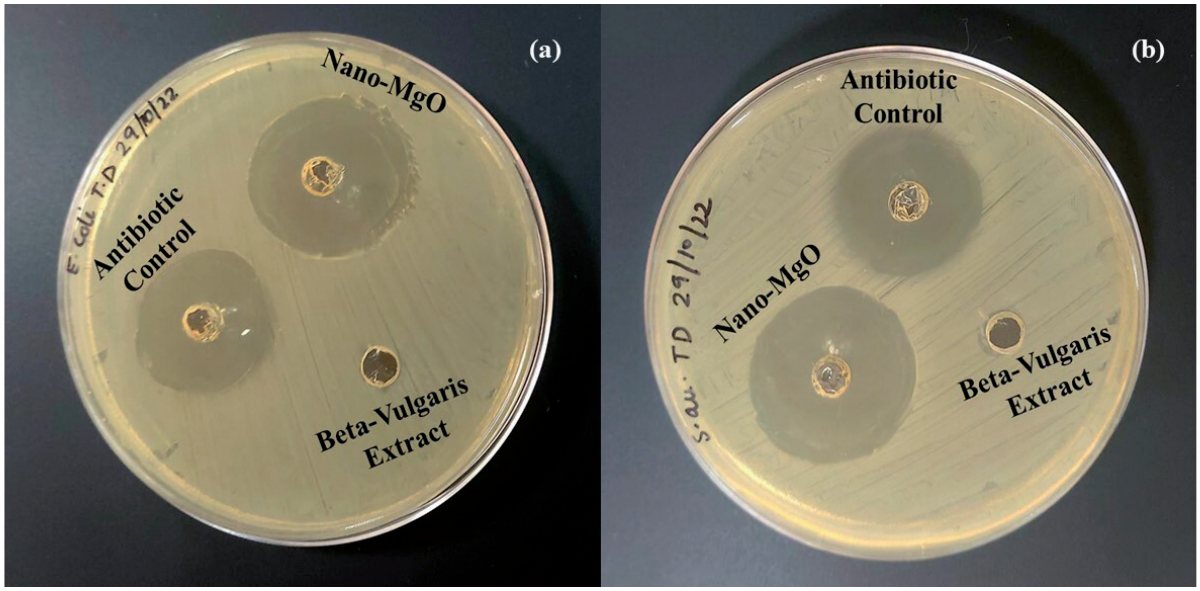

Fig. 8. Nano-MgO antimicrobial activity against a) E. Coli and; b) S. aureus.

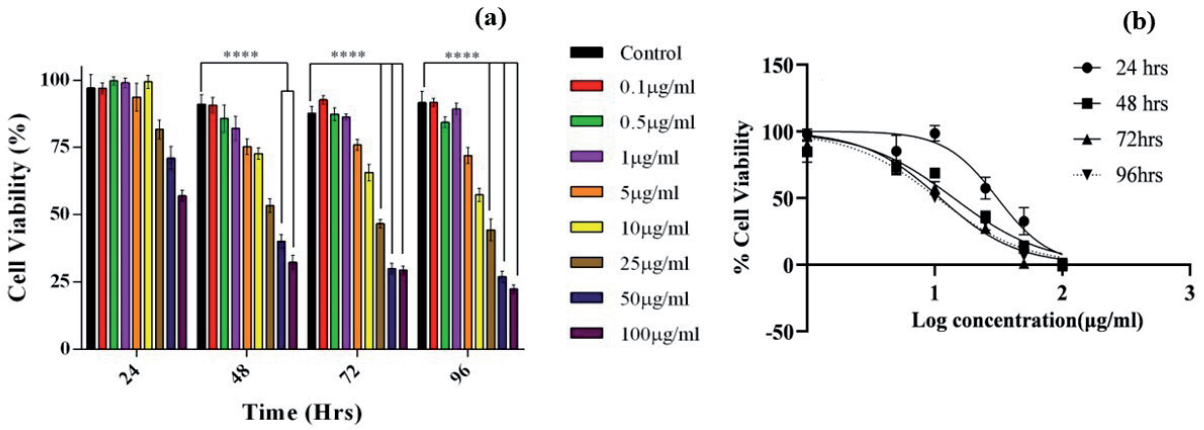

Fig. 9. The influence of Nano-MgO on cell viability a) cell viability; b) IC50 values Logarithmic-dose vs. response graph.

Conclusion

The current study suggests that magnesium oxide (MgO) nanostructures were successfully fabricated via a plant-mediated synthesis approach, utilizing an extract derived from *B. vulgaris*. The techniques such as FTIR, UV-Visible spectroscopy, XRD, SEM, TGA, and DCS were used to characterize nanoparticles. A color shift from red to green indicated that Nano-MgO was synthesized successfully. Mg-O functional groups were found using FTIR spectroscopy. The well-defined crystalline structures were confirmed by XRD signals. Using SEM, it was possible to see spherical Nano-MgO with an average size of 36.28 nm. These nanoparticles showed strong antibacterial and antioxidant activity. The adoption of the *B. vulgaris*-mediated approach, which makes the procedure more affordable and environmentally benign than chemical synthesis, is one of the study's key findings. In addition, *B. vulgaris* is widely accessible for a potential commercial-scale preparation of Nano-MgO, given that they are grown in many developing countries in large quantities. By using the procedure outlined in this paper, Nano-MgO with homogeneous size and shape can be produced for use in biotechnology and nanomedicine.

Acknowledgments

The authors thank Symbiosis International (Deemed University) for infrastructure and support. Authors thank Director and Deputy Director of Symbiosis School of Biological Sciences.

Conflict of Interest

The authors declare no conflict of interest.

References

1. NASROLLAHZADEH M., SAJADI S.M., SAJJADI M., ISSAABADI Z. An introduction to nanotechnology. InInterface science and technology. **28**, 1, **2019**.
2. HUSSAIN S., AZIZ I., WAQAS M., AHMAD T., AHMAD I., TAHIR M.B., NAZIR A. Potential Antifungal and Antimicrobial Effects of Nano Zinc Oxide Particles Obtained from Cymbogobon citratus Leaf Extract Using Green Technology. Polish Journal of Environmental Studies. **32** (5), 4065, **2023**.
3. NIKALJE A.P. Nanotechnology and its applications in medicine. Medicinal Chemistry. **5** (2), 081, **2015**.
4. KHAN I., SAEED K., KHAN I. Nanoparticles: Properties, applications, and toxicities. Arabian Journal of Chemistry. **12** (7), 908, **2019**.
5. JAMKHANDE P.G., GHULE N.W., BAMER A.H., KALASKAR M.G. Metal nanoparticles synthesis: An overview on methods of preparation, advantages and disadvantages, and applications. Journal of drug delivery science and technology. **53**, 101174, **2019**.
6. JEEVANANDAM J., CHAN Y.S., DANQUAH M.K. Biosynthesis of metal and metal oxide nanoparticles. ChemBioEng Reviews. **3** (2), 55, **2016**.
7. HAJIPOUR M.J., FROMM K.M ASHKARRAN A.A., DE ABERASTURI D.J., DE LARRAMENDI I.R., ROJO T., SERPOOSHAN V., PARAK W.J., MAHMOUDI M. Antibacterial properties of nanoparticles. Trends in biotechnology. **30** (10), 499, **2012**.
8. SANTOS C.S., GABRIEL B., BLANCHY M., MENES O., GARCÍA D., BLANCO M., ARCONADA N., NETO V. Industrial applications of nanoparticles – a prospective overview. Materials Today: Proceedings. **2** (1), 456, **2015**.
9. OSKAM G. Metal oxide nanoparticles: synthesis, characterization and application. Journal of sol-gel science and technology. **37**, 161, **2006**.
10. NIKOLOVA M.P., CHAVALI M.S. Metal oxide nanoparticles as biomedical materials. Biomimetics. **5** (2), 27, **2020**.
11. ABBAS M., HUSSAIN T., IQBAL J., REHMAN A.U., ZAMAN M.A., JILANI K., NAZIR A. Synthesis of silver nanoparticle from Allium sativum as an eco-benign agent for biological applications. Polish Journal of Environmental Studies, **31** (1), 533, **2022**.
12. RAJESHKUMAR S., BHARATH L.V. Mechanism of plant-mediated synthesis of silver nanoparticles–a review on biomolecules involved, characterisation and antibacterial activity. Chemico-biological interactions. **273**, 219, **2017**.
13. JANNAT M., KIRAN S., YOUSAF S., GULZAR T., IQBAL S. Potential Antifungal Effects of D. malabarica Assisted Zinc Oxide and Silver Nanoparticles against Sheath Blight Disease of Rice Caused by Rhizoctonia solani. Polish Journal of Environmental Studies **31** (5), **2022**.
14. CAI L., CHEN J., LIU Z., WANG H., YANG H., DING W. Magnesium oxide nanoparticles: effective agricultural antibacterial agent against Ralstonia solanacearum. Frontiers in microbiology. **9**, 790, **2018**.
15. SEZER N., EVIS Z., KAYHAN S.M., TAHMASEBIFAR A., KOÇ M. Review of magnesium-based biomaterials and their applications. Journal of magnesium and alloys. **6** (1), 23, **2018**.
16. DA SILVA B.L., CAETANO B.L., CHIARI-ANDRÉO B.G., PIETRO R.C., CHIAVACCI L.A. Increased antibacterial activity of ZnO nanoparticles: Influence of size and surface modification. Colloids and Surfaces B: Biointerfaces. **177**, 440, **2019**.
17. FERNANDES M., RB SINGH K., SARKAR T., SINGH P., PRATAP SINGH R. Recent applications of magnesium oxide (MgO) nanoparticles in various domains. Advanced Materials Letters. **11** (8), 1, **2020**.
18. ALFARO A., LEÓN A., GUAJARDO-CORREA E., REUQUEN P., TORRES F., MERY M., SEGURA R., ZAPATA P.A., ORIHUELA P.A. MgO nanoparticles coated with polyethylene glycol as carrier for 2-Methoxyestradiol anticancer drug. PLoS One. **14** (8), 0214900, **2019**.
19. BIANCARDI E., MCGRATH J.M., PANELLA L.W., LEWELLEN R.T., AMP STEVANATO P. Sugar beet. Root and tuber crops. 173, **2010**.
20. TRYCH U., BUNIOWSKA-OLEJNIK M., MARSZAŁEK K. Bioaccessibility of betalains in beetroot (*Beta vulgaris* L.) juice under different high-pressure techniques. Molecules. **27** (20), 7093, **2022**.
21. DESSEVA I., STOYANOVA M., PETKOVA N., MIHAYLOVA D,. Red beetroot juice phytochemicals

bioaccessibility: An in vitro approach. Polish Journal of Food and Nutrition Sciences. **70** (1), **2020**.
22. BINDHU M.R., UMADEVI M., MICHEAL M.K., ARASU M.V., AL-DHABI N.A. Structural, morphological, and optical properties of MgO nanoparticles for antibacterial applications. Materials Letters. **166**, 19, **2016**.
23. JOHN SUSHMA N., PRATHYUSHA D., SWATHI G., MADHAVI T., DEVA PRASAD RAJU B., MALLIKARJUNA K., KIM H.S. Facile approach to synthesize magnesium oxide nanoparticles by using Clitoria ternatea—characterization and in vitro antioxidant studies. Applied Nanoscience. **6**, 437, **2016**.
24. MAJI J., PANDEY S., BASU S. Synthesis and evaluation of antibacterial properties of magnesium oxide nanoparticles. Bulletin of Materials Science. **43**, 1, **2020**.
25. BAINSAL N., KAUR S., MALLAN S. Pharmacognostical, Physicochemical and Phytochemical studies of different varieties of Beet root grown in Punjab. Research Journal of Pharmacy and Technology. **14** (3), 1689, **2021**.
26. NUGRAHA S.E., NASUTION E.S., SYAHPUTRA RA. Investigation of phytochemical constituents and cardioprotective activity of ethanol extract of beetroot (Beta vulgaris. L) on doxorubicin induced toxicity in rat. **2020.**
27. KOU J., VARMA R.S. Beet juice utilization: Expeditious green synthesis of noble metal nanoparticles (Ag, Au, Pt, and Pd) using microwaves. RSC advances. **2** (27), 10283, **2012**.
28. KUMAR M.P., SURESH D., NAGABHUSHANA H., SHARMA S.C. Beta vulgaris aided green synthesis of ZnO nanoparticles and their luminescence, photocatalytic and antioxidant properties. The European Physical Journal Plus. **130** (6), 109, **2015**.
29. WONG C.W., CHAN Y.S., JEEVANANDAM J., PAL K., BECHELANY M., ELKODOUS M., EL-SAYYAD G.S. Response surface methodology optimization of mono-dispersed MgO nanoparticles fabricated by ultrasonic-assisted sol–gel method for outstanding antimicrobial and antibiofilm activities. Journal of Cluster Science. **31**, 367, **2020**.
30. HANEEFA M.M. Green synthesis characterization and antimicrobial activity evaluation of manganese oxide nanoparticles and comparative studies with salicylalchitosan functionalized nanoform. Asian Journal of Pharmaceutics (AJP). **11** (01), **2017**.
31. HIRPHAYE B.Y., BONKA N.B., TURA A.M., FANTA G.M. Biosynthesis of magnesium oxide nanoparticles using Hagenia abyssinica female flower aqueous extract for characterization and antibacterial activity. Applied Water Science. **13** (9), 175, **2023**.
32. SOMANATHAN T., KRISHNA V.M., SARAVANAN V., KUMAR R., KUMAR R. MgO nanoparticles for effective uptake and release of doxorubicin drug: pH sensitive controlled drug release. Journal of Nanoscience and Nanotechnology. **16** (9), 9421, **2016**.
33. AMMULU M.A., VINAY VISWANATH K., GIDUTURI A.K., VEMURI P.K., MANGAMURI U., PODA S. Phytoassisted synthesis of magnesium oxide nanoparticles from Pterocarpus marsupium rox.b heartwood extract and its biomedical applications. Journal of Genetic Engineering and Biotechnology. **19**, 1, **2021**.
34. SAIED E., EID A.M., HASSAN S.E., SALEM S.S., RADWAN A.A., HALAWA M., SALEH F.M., SAAD H.A., SAIED E.M., FOUDA A. The catalytic activity of biosynthesized magnesium oxide nanoparticles (Mgo-nps) for inhibiting the growth of pathogenic microbes, tanning effluent treatment, and chromium ion removal. Catalysts. **11** (7), 821, **2021**.
35. DOBRUCKA R. Synthesis of MgO nanoparticles using Artemisia abrotanum herbal extract and their antioxidant and photocatalytic properties. Iranian Journal of Science and Technology, Transactions A: Science. **42**, 547, **2018**.
36. SUTAPA I.W., WAHAB A.W., TABA P., L.A NAFIE N. Synthesis and structural profile analysis of the MgO nanoparticles produced through the sol-gel method followed by annealing process. Oriental Journal of Chemistry. **34** (2), 1016, **2018**.
37. BALAMURUGAN S., ASHNA L., PARTHIBAN P. Synthesis of nanocrystalline MgO particles by combustion followed by annealing method using hexamine as a fuel. Journal of Nanotechnology. 2014, **2014**.
38. OGUNYEMI S.O., ZHANG F., ABDALLAH Y., ZHANG M., WANG Y., SUN G., QIU W., LI B. Biosynthesis and characterization of magnesium oxide and manganese dioxide nanoparticles using Matricaria chamomilla L. extract and its inhibitory effect on Acidovorax oryzae strain RS-2. Artificial cells, nanomedicine, and biotechnology. **47** (1), 2230, **2019**.
39. THARANI K., CHRISTY A.J., SAGADEVAN S., NEHRU L.C. Fabrication of Magnesium oxide nanoparticles using combustion method for a biological and environmental cause. Chemical Physics Letters. **763**, 138216, **2021**.
40. ABINAYA S., KAVITHA H.P., PRAKASH M., MUTHUKRISHNARAJ A. Green synthesis of magnesium oxide nanoparticles and its applications: A review. Sustainable Chemistry and Pharmacy. **19**, 100368, **2021**.
41. AKRAM M.W., FAKHAR-E-ALAM M., ATIF M., BUTT A.R., ASGHAR A., JAMIL Y., ALIMGEER K.S WANG Z.M. In vitro evaluation of the toxic effects of MgO nanostructure in Hela cell line. Scientific reports. **8** (1), 4576, **2018**.
42. ALARFAJ N.A., AMINA M., AL MUSAYEIB N.M., EL-TOHAMY M.F., ORABY H.F., BUKHARI S.I., MOUBAYED N.M. Prospective of green synthesized Oleum cumini Oil/PVP/MgO bio nanocomposite film for its antimicrobial, antioxidant, and anticancer applications. Journal of Polymers and the Environment. **28**, 2108, **2020**.